Available online at www.eccomasproceedia.org
Eccomas Proceedia UNCECOMP (2017) 76-89

ECCOMAS
Proceedia

UNCECOMP 2017
2nd ECCOMAS Thematic Conference on
Uncertainty Quantification in Computational Sciences and Engineering
M. Papadrakakis, V. Papadopoulos, G. Stefanou (eds.)
Rhodes Island, Greece, 15–17 June 2017

RELIABILITY PREDICTION OF FATIGUE DAMAGE ACCUMULATION ON WIND TURBINE SUPPORT STRUCTURES

K. Tatsis[1], E. Chatzi[1] and E. Lourens[2]

[1]ETH Zürich, Institute of Structural Engineering
Stefano-Franscini-Platz 5, 8093 Zürich, Switzerland
e-mail: tatsis@ibk.baug.ethz.ch , chatzi@ibk.baug.ethz.ch

[2] Delft University of Technology, Faculty of Civil Engineering and Geosciences
Stevinweg 1, 2628 CN Delft, The Netherlands
e-mail: e.lourens@tudelft.nl

Keywords: Wind turbine, Structural monitoring, Input-state estimation, Response identification, Fatigue damage, Reliability.

Abstract. *The evaluation of fatigue damage accumulation on wind turbine support structures under operational conditions is heavily influenced by a number of uncertainties. These uncertainties may, firstly, be attributed to the highly variable and complex environmental loads, and secondly, to the unavoidable modelling errors which mainly originate from the inherent randomness in both material properties and fatigue resistance of structural components. It is therefore essential that assessment of fatigue life is carried out within a probabilistic framework; one that accounts for the stochastic nature of the phenomenon. The present study proposes a strategy for real-time reliability prediction of accumulated fatigue damage on wind turbine support structures by taking into account the above-mentioned uncertainties. To this end, the availability of structural monitoring information for the identification of the global response on wind-turbine support structures is exploited in order to address the discrepancies between actual and predicted damage accumulation. This is carried through utilization of an augmented version of the Kalman filter, which is capable of jointly estimating the response and the unknown inputs of the structure while relying on a limited number of noisy observations and a presumably uncertain model of the real system. A fixed-lag smoother is further deployed for the attenuation of the estimation error in an on-line mode and the smoothed stochastic estimates of the response are propagated over the model at the level of stresses. The accumulated damage along with the corresponding reliability level is finally predicted using a stochastic nonstationary fatigue damage model. The proposed scheme is demonstrated via implementation on the NREL 5.0 MW wind turbine under different operational conditions, on the basis of dummy vibration data generated via the FAST software.*

Peer-review under responsibility of the organizing committee of UNCECOMP 2017.
doi: 10.7712/120217.5353.17130

1 INTRODUCTION

Fatigue is regarded as a critical and highly-uncertain factor for wind turbine structures, where it is essential to ensure a certain life span under irregular and constantly varying operational and environmental conditions. Conventionally, fatigue life predictions are conducted on the basis of numerical simulations in conjunction with the information provided from historical metocean data. In the wake of recent advancements in Structural Health Monitoring technologies and methodologies, significant attention has been redirected to vibration-based approaches for fatigue estimation [1], particularly to what pertains to response prediction under unknown inputs.

Although fatigue has been vastly and exhaustively investigated under different perspectives [2], not many studies have been relied on a probabilistic framework. In recent years, an attempt has been made to approach damage accumulation due to fatigue as a stochastic process [3]. To account for the randomness in both the loading process and fatigue resistance of materials, Shen et al. [4] established a probabilistic model of fatigue damage based on the distribution of stress amplitudes. Despite the efficiency in obtaining the distribution of fatigue damage, the approach in [4] is not appropriate for real-time applications. On the contrary, Rathod et al. [5] proposed a more universal methodology for the stochastic modelling of damage accumulation under multilevel loading, which may be easily tailored to an online framework. In a more recent work and in the field of wind turbine structures, Thöns et al. [6] conducted a sensitivity study for fatigue limit state on the basis on the Spearman rank coefficient. The outcome of the study in [6] provides a useful insight into the most influential sources of uncertainty in fatigue damage. Within the same context, Thöns et al. [7] conducted a quantitative study for the value of structural health monitoring towards the integrity management of fatigue deteriorating structural systems.

In what concerns the real-time state estimation of systems with unknown inputs, a variety of methods is currently available. The primary step was taken by Kitanidis [8] through the development of a linear state estimator in the presence of unknown inputs. Under this perspective, Gillijns et al. [9] proposed an unbiased minimum-variance filter for the joint input-state estimation of linear time invariant systems. Although optimal in terms of second order statistics, the estimator in [9] was proven to be susceptible to numerical issues when the number of measurements is larger than the order of the system. This was recently alleviated by Lourens et al. [10] with an extension of the previously mentioned algorithm. An alternative for the dual state and input estimation of structural systems was implemented also by Lourens et al. [11], using an augmented version of the standard Kalman filter. To improve the poor performance of the latter when acceleration-only measurements are employed, Naets et al. [12] proposed a stabilized version of the augmented Kalman filter by using dummy displacement measurements. Finally, in more recent years Azam et al. [13] suggested a dual implementation of the Kalman filter in order to resolve the numerical issues that arise in the augmented formulation of input-state estimation problem.

This study presents a vibration-based probabilistic framework for fatigue assessment on wind turbine structures accounting for uncertainties in the level of the structural model, the estimated stresses time histories and the employed fatigue model. The paper is organized as follows: in Section 2 the mathematical formulation of the response estimation problem for systems with unknown inputs is established. This is carried out using the augmented form of the Kalman filter which is further enhanced with a fixed-lag smoother for the attenuation of the underlying model uncertainty and the improvement of state estimates. In Section 3, the stochastic framework for fatigue assessment is presented. This comprises a non-stationary fatigue model capable of

capturing the expected value and variance of fatigue damage as well as their evolution in time as a function of the loading history. Finally, the implementation of the proposed approach is illustrated in Section 4 by means of an application to a wind turbine support structure on the basis of simulated measurement data.

2 RESPONSE ESTIMATION

The starting point for the response estimation on wind turbine structures is the continuous-time system of equations of motion

$$\mathbf{M}\ddot{\mathbf{u}}(t) + \mathbf{C}\dot{\mathbf{u}}(t) + \mathbf{K}\mathbf{u}(t) = \mathbf{S}_p\mathbf{f}(t) \tag{1}$$

where $\mathbf{u}(t) \in \mathbb{R}^n$ denotes the displacement vector, $\mathbf{M}$, $\mathbf{C}$, $\mathbf{K} \in \mathbb{R}^{n\times n}$ are the mass, damping and stiffness matrices, $\mathbf{f}(t) \in \mathbb{R}^{n_\mathrm{p}}$ is the force vector, with n_p designating the number of input forces, and $\mathbf{S}_p \in \mathbb{R}^{n\times n_\mathrm{p}}$ is the corresponding selection matrix.

Upon introduction of the state vector $\mathbf{x}(t) = \mathrm{vec}\big([\dot{\mathbf{u}}(t)\ \mathbf{u}(t)]\big) \in \mathbb{R}^{2n}$, Eq. (1) may be transformed into the state equation and additionally fused with a measurement process in order to form the deterministic state-space model in the continuous-time domain. The latter can be further transferred, through temporal discretization, to the discrete-time domain, which yields the following stochastic state and observation equations

$$\mathbf{x}_{k+1} = \mathbf{A}\mathbf{x}_k + \mathbf{B}\mathbf{p}_k + \mathbf{w}_k \tag{2}$$

$$\mathbf{y}_k = \mathbf{G}\mathbf{x}_k + \mathbf{J}\mathbf{p}_k + \mathbf{v}_k \tag{3}$$

where it should be noted that Eqs. (2) and (3) are additionally supplemented with the zero-mean white noise processes $\mathbf{w}_k \in \mathbb{R}^{2n}$ and $\mathbf{v}_k \in \mathbb{R}^{n_y}$ that represent the system and measurement noise of covariance matrices $\mathbf{Q} \in \mathbb{R}^{2n\times 2n}$ and $\mathbf{R} \in \mathbb{R}^{n_y\times n_y}$, respectively.

In the absence of knowledge with respect to the driving forces of the system, the state-space model described in Eqs. (2) and (3) may be written in the augmented form. This is accomplished by supplementing the initial state vector with the input force vector in order to construct an augmented state vector as follows

$$\mathbf{z}_k = \begin{bmatrix}\mathbf{x}_k \\ \mathbf{p}_k\end{bmatrix} \tag{4}$$

To derive the system matrices of the augmented state-space, it is postulated that the evolution of the input dynamics may be captured by a random-walk process

$$\mathbf{p}_{k+1} = \mathbf{p}_k + \boldsymbol{\eta}_k \tag{5}$$

upon proper tuning of the random variable $\boldsymbol{\eta}_k \in \mathbb{R}^{n_p}$ which represents a zero-mean white Gaussian process with covariance matrix $\mathbf{S} \in \mathbb{R}^{n_p\times n_p}$. The augmented state and measurement equations may then be formulated as follows

$$\mathbf{z}_{k+1} = \mathbf{A}_\mathrm{a}\mathbf{z}_k + \boldsymbol{\zeta}_k \tag{6}$$

$$\mathbf{y}_k = \mathbf{G}_\mathrm{a}\mathbf{z}_k + \mathbf{v}_k \tag{7}$$

where the subscript$_\mathrm{a}$ denotes the augmented state-space matrices,

$$\mathbf{A}_\mathrm{a} = \begin{bmatrix} \mathbf{A} & \mathbf{B} \\ \mathbf{0} & \mathbf{I} \end{bmatrix}, \qquad \mathbf{G}_\mathrm{a} = \begin{bmatrix} \mathbf{G} & \mathbf{J} \end{bmatrix},$$

and $\boldsymbol{\zeta}_k = \mathrm{vec}\big(\begin{bmatrix} \mathbf{w}_k & \boldsymbol{\eta}_k \end{bmatrix} \big) \in \mathbb{R}^{2n+n_p}$ is the augmented noise vector with covariance matrix $\mathbf{Q}_\mathrm{a} \in \mathbb{R}^{2n+n_p \times 2n+n_p}$. Thereafter, both input and state estimation may be accomplished recursively through the standard Kalman filter operating on the augmented state-space formulation in two steps

Time update

$$\begin{aligned} \hat{\mathbf{z}}_{k+1|k} &= \mathbf{A}_\mathrm{a} \hat{\mathbf{z}}_{k|k} \\ \mathbf{P}_{k+1|k} &= \mathbf{A}_\mathrm{a} \mathbf{P}_{k|k} \mathbf{A}_\mathrm{a}^\mathrm{T} + \mathbf{Q}_\mathrm{a} \end{aligned} \tag{8}$$

Measurement update

$$\begin{aligned} \mathbf{K}_k &= \mathbf{P}_{k|k-1} \mathbf{G}_\mathrm{a}^\mathrm{T} \left(\mathbf{G}_\mathrm{a} \mathbf{P}_{k|k-1} \mathbf{G}_\mathrm{a}^\mathrm{T} + \mathbf{R} \right)^{-1} \\ \hat{\mathbf{z}}_{k|k} &= \hat{\mathbf{z}}_{k|k-1} + \mathbf{K}_k \left(\mathbf{y}_k - \mathbf{G}_\mathrm{a} \hat{\mathbf{z}}_{k|k-1} \right) \\ \mathbf{P}_{k|k} &= \mathbf{P}_{k|k-1} - \mathbf{K}_k \mathbf{G}_\mathrm{a} \mathbf{P}_{k|k-1} \end{aligned} \tag{9}$$

2.1 Smoothing and backward sampling

In the previous section, it was demonstrated how optimal *a priori* and *a posteriori* state and input estimates may be obtained on the basis of a limited number of response measurements. Due to the probabilistic origin of the Kalman filter, these state estimates are delivered in terms of the first two moments of their probability distribution, which essentially reflects the uncertainty associated with both the system dynamics and the measurement quality. An effective way of attenuating this uncertainty and improving the performance of the estimator is to further condition the forward results on posterior measurements via the so-called smoothing process.

Among the three basic classes of smoothers, that is fixed-point, fixed interval and fixed-lag smoothers, the latter is considered as the optimal estimator since, apart from allowing for processing delay, it is also tailored for on-line operation [14]. The aim of such a smoother is to provide the optimal state estimate at time $k-N$ conditioned on measurements up to and including time instant k. It is therefore required that N future measurements are available for the smoothed state estimation at time instant $k-N$.

Upon obtaining the state estimates at time k using the augmented Kalman filter, the fixed interval smoother is running backwards from k up to $k-N$ in order to provide the smoothed estimate of each state with delays between 0 and N. This process is summarized in four steps performed for $i = 2, \ldots, N+1$ at each time instant k as follows

Fixed-lag smoother

$$\begin{aligned} \mathbf{L}_{k,i} &= \mathbf{P}_k^{0,i-1} \mathbf{G}^\mathrm{T} \left(\mathbf{G} \mathbf{P}_k^{0,0} \mathbf{G}_k^\mathrm{T} + \mathbf{R}_k \right)^{-1} \\ \hat{\mathbf{z}}_{k+1-i|k} &= \hat{\mathbf{z}}_{k+2-i|k} + \mathbf{L}_{k,i} \left(\mathbf{y}_k - \mathbf{G} \mathbf{z}_{k|k-1} \right) \\ \mathbf{P}_{k+1}^{0,i} &= \mathbf{P}_k^{0,i-1} \left(\mathbf{A} - \mathbf{L}_{k,0} \mathbf{G} \right)^\mathrm{T} \\ \mathbf{P}_{k+1}^{i,i} &= \mathbf{P}_k^{i-1,i-1} - \mathbf{P}_k^{0,i-1} \mathbf{G}^\mathrm{T} \mathbf{L}_{k,i}^\mathrm{T} \mathbf{A}^\mathrm{T} \end{aligned} \tag{10}$$

It should be noted that for $i = 1$ the matrix $\mathbf{L}_{k,i}$ is equal to the Kalman gain and the above process represents the measurement update of the standard Kalman filter. Accordingly, the covariance matrix $\mathbf{P}_k^{0,0}$ designates the *a priori* estimate error covariance while in the general case the covariance matrices $\mathbf{P}_k^{i,j}$ are defined as

$$\mathbf{P}_k^{i,j} = \mathbb{E}\left[\left(\mathbf{z}_{k-j} - \hat{\mathbf{z}}_{k-j,k-1}\right)\left(\mathbf{z}_{k-i} - \hat{\mathbf{z}}_{k-i,k-1}\right)^{\mathrm{T}}\right] \tag{11}$$

Once the smoothed state and input estimates at time instant $k - N$ are obtained, it may easily be deduced from Eqs. (10) that the final state estimate is delivered as a Gaussian distribution with mean and variance

$$\mathbb{E}\left[\mathbf{z}_{k-N}|\mathbf{y}_1, \ldots, \mathbf{y}_k\right] = \hat{\mathbf{z}}_{k-N+1|k} + \mathbf{L}_{k,N+1}\left(\mathbf{y}_k - \mathbf{G}\hat{\mathbf{z}}_{k|k-1}\right) \tag{12}$$

$$\mathbb{E}\left[\left(\mathbf{z}_{k-N} - \hat{\mathbf{z}}_{k-N,k}\right)\left(\mathbf{z}_{k-N} - \hat{\mathbf{z}}_{k-N,k}\right)^{\mathrm{T}}\right] = \mathbf{P}_k^{N,N} - \mathbf{P}_k^{0,N}\mathbf{G}^{\mathrm{T}}\mathbf{L}_{k,N}^{\mathrm{T}}\mathbf{A}^{\mathrm{T}} \tag{13}$$

where every quantity on the right-hand side is obtained through the last step of smoothing process. Within the context of fatigue assessment, this uncertainty in state estimates may be propagated over the model at the level of stresses and subsequently quantified through the backward sampling of the stress time histories in order to account for the modelling and measurement uncertainties.

3 FATIGUE DAMAGE

Fatigue damage accumulation is a stochastic process characterized by several uncertainties. These uncertainties are associated with a number of sources, such as material properties, modeling errors and loading conditions among others. Under this perspective, it is essential that damage accumulation is treated within a probabilistic framework, one that is able to account for the stochastic nature of the phenomenon. In so doing, the present study is based on the premise of non-stationary and normally distributed damage accumulation process

$$D(t) \sim N\left(\mu_D(t), \sigma_D^2(t)\right) \tag{14}$$

with $\mu_D(t)$ and $\sigma_D^2(t)$ denoting the time-varying mean and variance respectively. The elaboration of this assumption is presented in three steps through the following sections.

3.1 Model of damage accumulation

A common practice for the evaluation of fatigue damage in steel structures is the linear accumulation rule, also known as Palmgen-Miner rule [15, 16], whereby damage at a given stress level is defined as the ratio of operational cycles to the number of failure cycles. For varying stress level, this is formulated as follows

$$D = \sum_{j=1}^{k} D_j = \sum_{j=1}^{k} \frac{n\left(\Delta\sigma_j\right)}{N_f\left(\Delta\sigma_j\right)} \tag{15}$$

where $n\left(\Delta\sigma_j\right)$ is the number of cycles with stress amplitude $\Delta\sigma_j$, $N_f\left(\Delta\sigma_j\right)$ denotes the number of cycles to failure at stress level $\Delta\sigma_j$ and k is the number of stress ranges contained in the examined time history. In the case of directly measured or estimated strain/stress time histories,

the number of cycles at stress amplitude $\Delta\sigma_j$ may be determined using counting techniques. Among others, the rainflow counting algorithm, which is thoroughly described in [17] and employed in this study as well, constitutes the most accurate and commonly used method in fatigue analysis. Finally, the relationship between fatigue life in terms of cycles N_f and stress range $\Delta\sigma$ is obtained by the well-known $S-N$ curve [18] which is expressed by

$$N_f \Delta\sigma^m = A \tag{16}$$

where A represents a fatigue strength constant and m denotes the slope of the curve, with both variables being material dependent. Combining Eq. (15) and the $S-N$ curve model described by Eq. (16), the expression of damage accumulation for multi-stress levels may be written as

$$D = \sum_{j=1}^{k} C \left(\Delta\sigma_j\right)^m n \left(\Delta\sigma_j\right) \tag{17}$$

with C denoting the reciprocal of fatigue strength constant A.

3.2 Distribution of fatigue damage

In establishing a probabilistic representation of damage accumulation, fatigue life is considered to be described by a probabilistic $S-N$ curve, as illustrated in Fig. 1. In practice, this is accomplished by treating the failure cycles N_f of each stress level as a random variable that follows a certain distribution. Since fatigue life of components under constant or random amplitude stress conditions may be adequately represented via normal or log-normal distributions, as underlined by Wu et al. [19], it is assumed that the number of cycles to failure at a certain stress level is normally distributed

$$f_n\left(N_f\right) = \frac{1}{\sigma_{N_f}\sqrt{2\pi}} \exp\left(-\frac{1}{2}\left(\frac{N_f - \mu_{N_f}}{\sigma_{N_f}}\right)^2\right) \tag{18}$$

with mean μ_{N_f} and standard deviation σ_{N_f}. The corresponding distribution of damage accumulation at the same stress level may then be derived through the one-to-one transformation of Eq. (18). The latter requires the functional relationship $N_f = h\left(D\right)$ between failure life N_f and damage accumulation D, which may be obtained through evaluation of Eq. (17) at failure

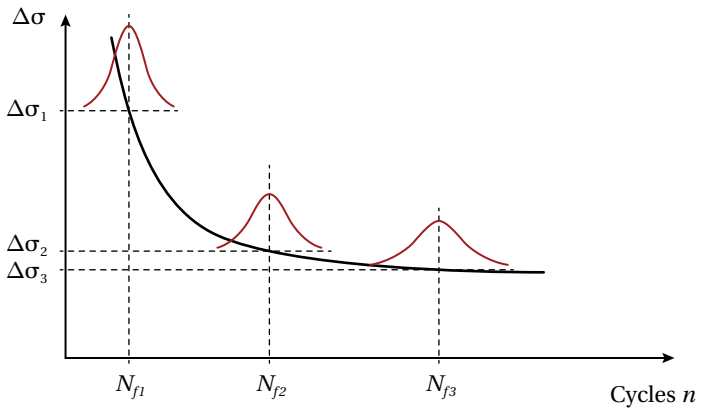

Figure 1: Probabilistic $S-N$ curve

life for a single stress level. Thereafter, the probability density function of cumulative damage D may be calculated through the differentiation of its cumulative distribution as shown below

$$\begin{aligned} f_D(D) &= \frac{d}{dD} F_D(D) \\ &= \frac{D}{dD} F_n\left(h^{-1}(D)\right) \\ &= \frac{D}{dD}\left(\int_{-\infty}^{h^{-1}(D)} f_n\left(N_f\right) dN_f\right) \\ &= \frac{dh^{-1}(D)}{dD} f_n\left(h^{-1}(D)\right) \\ &= \frac{dN_f}{dD} f_n\left(N_f\right) \end{aligned} \tag{19}$$

where $dN_f/dD = 1/s$ with $s = C\left(\Delta\sigma\right)^m$ denoting the slope of the $S-N$ curve at the stress level $\Delta\sigma$. Substituting in Eq. (19) and making use of Eq. (17) for a single stress level and Eq. (18), the probability density function of D may be written as follows

$$f_D(D) = \frac{1}{s\sigma_{N_f}\sqrt{2\pi}} \exp\left(-\frac{1}{2}\left(\frac{D - s\mu_{N_f}}{s\sigma_{N_f}}\right)^2\right) \tag{20}$$

where it may be observed that fatigue damage follows a normal distribution as well

$$D\left(N_f\right) \sim N\left(s\mu_{N_f}, s\sigma_{N_f}\right) \tag{21}$$

with mean $s\mu_{N_f}$ and standard deviation $s\sigma_{N_f}$.

3.3 Evolution of variance

As illustrated in Fig. 1, fatigue life follows an increasing trend in variability as stress level decreases, thus resulting in low variability of failure cycles at high stress conditions and higher variability at low stress levels. Additionally, as demonstrated by Wang et al. [20], damage accumulation at constant stress level exhibits a monotonically increasing variability as usage cycles increase. This second source of variability is graphically depicted in Fig. 2, where it

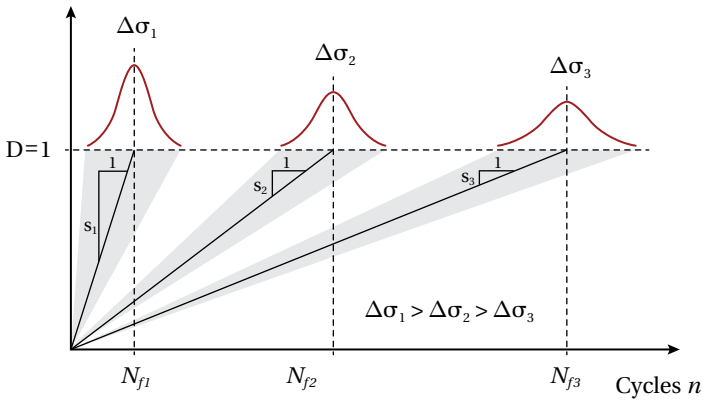

Figure 2: Evolution of variance for different stresses

may be inferred that the initial stage is represented by zero usage cycles and zero variability for all stress levels. Subsequently, as the number of usage cycles at a certain stress level increases, the variability is accordingly increasing until it reaches a certain value σ_{N_f} at failure life. This trend may be geometrically interpreted, as elaborated by Rathod et al. [5], and captured through the rate of change of the standard deviation r_σ, given by

$$r_\sigma = \frac{\sigma_{N_f}}{N_f} \tag{22}$$

Subsequently, the standard deviation of the loading cycles n may be derived from the product of the rate of change and the number of cycles n, given by the following expression

$$\sigma_n = r_\sigma n = \left(\frac{\sigma_{N_f}}{N_f}\right) n \tag{23}$$

Considering finally that the damage index is related to the number of cycles via the slope $s = C\left(\Delta\sigma\right)^m$ of the $S-N$ curve, the standard deviation of cumulative damage may be written as follows

$$\sigma_D = \left(\frac{\sigma_{N_f}}{N_f}\right) ns = C\left(\Delta\sigma\right)^m n \left(\frac{\sigma_{N_f}}{N_f}\right) \tag{24}$$

Although the above formula represents the variability in damage due to single stress-level condition, it can be readily extended to account for the variability in damage accumulation under multi-level stress conditions, as graphically presented in Fig. 3. In so doing, it is assumed that damage accumulation at each stress level bears an independent stochastic contribution to the total variability of damage accumulation which is given by

$$\sigma_D = \sqrt{\sum_{j=1}^{k} \left(C\left(\Delta\sigma_j\right)^m n_j \left(\frac{\sigma_{N_{f_j}}}{N_{f_j}}\right)\right)^2} \tag{25}$$

where N_{f_j} denotes the cycles to failure at stress level $\Delta\sigma_j$ and $\sigma_{N_{f_j}}$ the corresponding standard deviation.

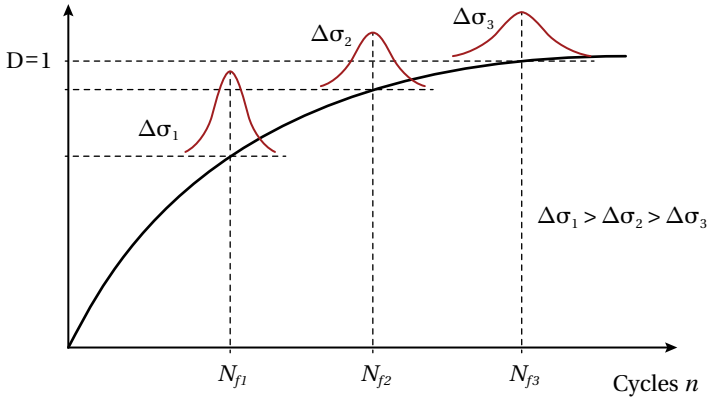

Figure 3: Damage accumulation for multi-stress loading

3.4 Reliability prediction

Based on the above probabilistic model for fatigue damage accumulation, which relies on the assumption of normally distributed usage and failure cycles, the reliability of a structural component with respect to fatigue damage may be calculated through the limit state function

$$Z(n) = D_c - D(n) \tag{26}$$

where D_c is the critical damage with $\mathbb{E}[D_c] = 1$ and $Z(n) = 0$ describes the limit state that separates the safe domain, for which $Z(n) > 0$, from the failure region where $Z(n) < 0$. Thereafter, the reliability is calculated on the basis of the limit state function as follows

$$\begin{aligned} R &= P(Z(n) > 0) \\ &= 1 - P(Z(n) \leq 0) \\ &= 1 - \Phi\left(-\frac{\mu_{D_c} - \mu_D}{\sqrt{\sigma_{D_c}^2 + \sigma_D^2}}\right) \end{aligned} \tag{27}$$

with μ_D and σ_D denoting the mean and the standard deviation of damage accumulation while μ_{D_c}, σ_{D_c} designate the mean the standard deviation of threshold damage.

Thereafter, substitution of Eqs. (17) and (25) into Eq. (27) yields the reliability index of a structural component under multi-level stress conditions as given below

$$R = 1 - \Phi\left(-\frac{\mu_{D_c} - \sum_{j=1}^{k} C\left(\Delta\sigma_j\right)^m n\left(\Delta\sigma_j\right)}{\sqrt{\sigma_{D_c}^2 + \sum_{j=1}^{k}\left(C\left(\Delta\sigma_j\right)^m n\left(\Delta\sigma_j\right)\left(\sigma_{N_{f_j}}/N_{f_j}\right)\right)^2}}\right) \tag{28}$$

where it should be noted that the variability of threshold damage σ_{D_c} at failure life, i.e. when $n = N_f$, is equal to the variability of damage accumulation σ_D, given by Eq. (25). This is also implied from Fig. 2 where it is shown that the variability of damage follows a monotonically increasing trend until it reaches the value of threshold damage at failure level.

4 RESULTS

The demonstration of the proposed scheme for reliability prediction of fatigue damage accumulation is carried out through an application to the NREL 5.0 MW land-based wind turbine, whose features are in detail presented by Jonkman et al. [21]. To investigate the fatigue limit state (FLS), the considered structure is modelled using the FAST v8 software platform for the generation of artificial measurements from aero-servo-elastic simulations in operational conditions. A total of two hundred simulations, each with a duration of ten minutes, is used for this purpose. Each simulation is performed at a mean wind speed sampled from a Weibull distribution with mean equal to 10 m/s and a turbulence intensity derived from a log-normal distribution conditioned on the previously sampled mean wind speed.

To enable the implementation of the proposed approach in a long-term period, the structural response is assumed to be measured with sensors appropriate for continuous and permanent

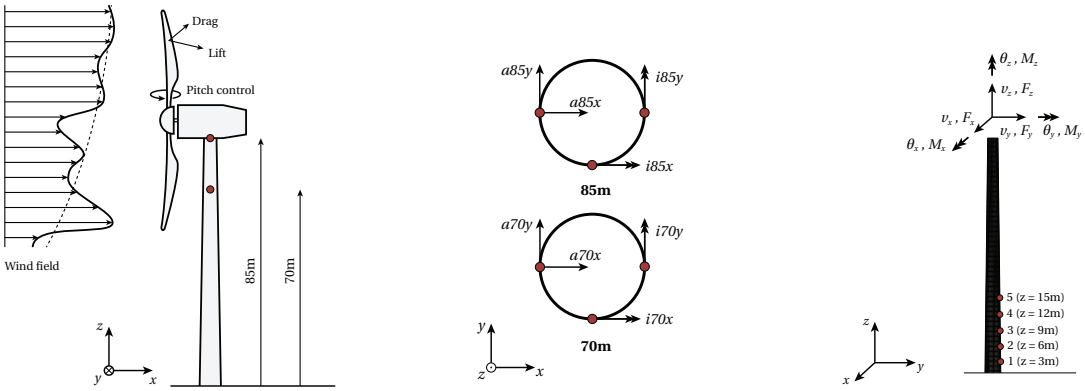

(a) Simulated wind turbine (b) Sensor configuration (c) Critical locations

Figure 4: Overview of the sensor locations, the finite element model of the tower and the critical locations

monitoring. In this study, availability of acceleration and inclination measurements is assumed, whose adopted configuration is depicted in Figs. 4(a) and 4(b). Their number and location on the structure are determined by the stability and observability conditions, in accordance with the number of inputs to be identified and their corresponding locations. These inputs are considered to be the interface forces between the tower top and the nacelle, as illustrated in Fig. 4(c).

To additionally account for modelling errors, a stochastic Finite Element (FE) model of the wind turbine structure is employed for the solution of the inverse problem. Namely, while the forward process for the data generation is carried out with a perfectly known deterministic model, the one implemented in FAST, the identification part is performed with a perturbed FE model. This is a refined shell-element model, reduced with a component mode synthesis technique, that involves a randomness in the material properties, introduced at the level of the constitutive matrix $\mathbf{C}$ as follows

$$\mathbf{C} = \mathbf{C}_0\big(\alpha + f(\mathbf{x})\big) \tag{29}$$

where α, equal to 0.95, is a perturbation factor for the mean value of $\mathbf{C}$ which is denoted by $\mathbf{C}_0$ and $f(\mathbf{x})$ is a zero-mean stochastic process which is herein assumed to be log-normally distributed with standard deviation $2 \cdot 10^{10}$ N/m^2. Within this context, the stochastic stiffness matrix of an element (e) may be expressed on the basis of the principle of virtual work as

$$\mathbf{k}^{(\mathrm{e})} = \mathbf{k}_0^{(e)} + \Delta\mathbf{k}_{\mathrm{s}}^{(\mathrm{e})} = \int_{V^{(\mathrm{e})}} \mathbf{B}^{(\mathrm{e})} \alpha \mathbf{C}_0 \mathbf{B}^{(\mathrm{e})} dV^{(\mathrm{e})} + \int_{V^{(\mathrm{e})}} \mathbf{B}^{(\mathrm{e})} \mathbf{C}_0 f^{(\mathrm{e})}(\mathbf{x}) \mathbf{B}^{(\mathrm{e})} dV^{(\mathrm{e})} \tag{30}$$

where $\mathbf{k}_0^{(e)}$ is the perturbed deterministic part and $\Delta\mathbf{k}_{\mathrm{s}}^{(\mathrm{e})}$ denotes the fluctuating part. For the sake of completeness, it should be noted that $V^{(\mathrm{e})}$ is the volume of element (e) and $\mathbf{B}^{(\mathrm{e})}$ represents the deformation matrix.

The simulation measurements obtained from FAST are polluted with 3% white Gaussian noise and subsequently fed to the augmented Kalman filter which is operating along with the fixed-lag smoother for the dual input and state estimation of the perturbed model. The algorithm is initialized with a zero state vector, the measurement error covariance is obtained as a function of the noise level and the system error covariance is calculated on the basis of the L-curve, as shown in Fig. 5. The smoothed state estimates, which are delivered as Gaussian random

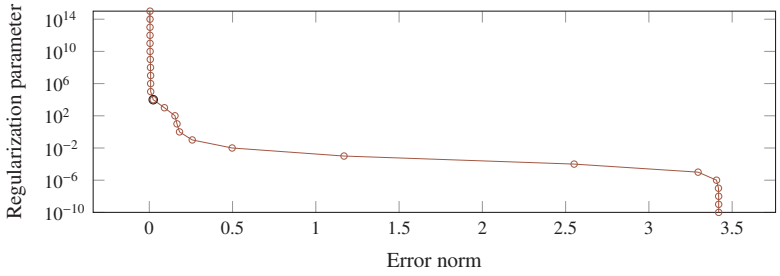

Figure 5: L-curve for the optimal choice of the regularization parameter

variables with mean and variance given by Eqs. (12) and (13), are finally propagated over the model in order to obtain the corresponding distributions of stress estimates at critical locations.

The expected value of stress time histories for locations 1 and 2 are illustrated in Fig. 6 and 7 respectively, along with their 95% confidence intervals for two different time frames of 100s and 5s. Although an erroneous model is used for the response identification, it is seen that the stress time histories are identified with a sufficiently high degree of accuracy. This may be primarily attributed to the capability of the filter to provide robust response estimates, when an erroneous model is deployed, at the expense of the input predictions and secondly to the smoothing effect which yields a substantial improvement on the peak estimates.

To quantify the uncertainty of the estimated stress time histories, which implicitly comprises all kinds of uncertainty associated with the FE model and the response measurements, the time histories are backwards sampled in a Monte Carlo framework and subsequently counted with the rainflow algorithm, yielding thus a stochastic representation of the stress cycle distribution. The latter is then processed with the fatigue model of Section 3 and produces the time-dependent distribution of damage accumulation. It should be noted that in the context of this study, the fatigue strength parameters are chosen such that a substantial part of the fatigue life of the structure is wasted throughout the simulation time.

The expected value of accumulated fatigue damage with respect to the number of usage cycles for the whole simulation time of two thousand minutes at locations 1 and 2 is depicted

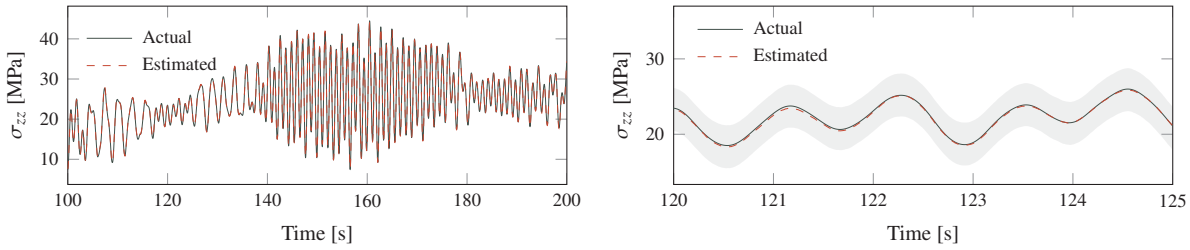

Figure 6: Actual and estimated stress time history with 95% confidence interval for location 1

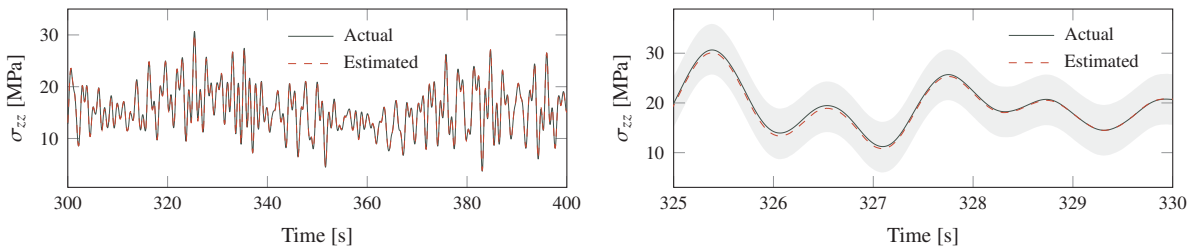

Figure 7: Actual and estimated stress time history with 95% confidence interval for location 2

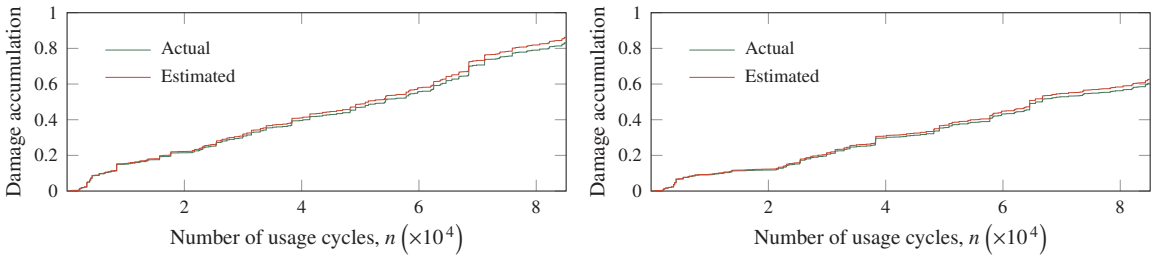

(a) location 1 (b) location 2

Figure 8: Expected value of fatigue damage accumulation on locations 1 and 2

in Fig. 8. As observed, the evolution of damage is identified with a high degree of accuracy, yet there is a small drift on the estimates which mainly stems from spurious cycles due to noise on measurements. The total damage accumulation for all five locations is presented in the bar-chart of Fig. 9, showing the sufficiently good agreement between actual and estimated values, with a 7% maximum error.

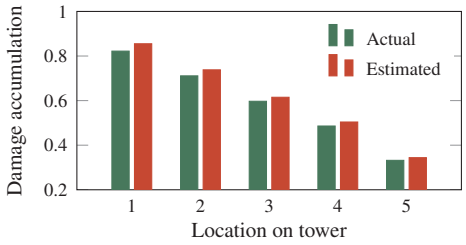

Figure 9: Expected value of accumulated fatigue damage on locations 1-5

Finally, the time-dependent reliability index of a structural component under the estimated stress conditions is evaluated on the basis of Eq. (28). Figure 10 shows the evolution of reliability with respect to the number of usage cycles for locations 1 and 2, where it is evident that reliability follows a decreasing trend as the number of usage cycles increases. As underlined in Section 3, the rate of change of the reliability index is dependent on the stress conditions, resulting to higher rate of loss for high-low cycles and accordingly to lower one for low stress levels. An additional information revealed from Fig. 10 pertains to the evolution of fatigue mechanisms. Namely, it may be deduced that the initial and highly reliable period represents the phase of crack initiation while the crack propagation period is indicated by loss of reliability. This implies that high stress-level conditions result in small crack initiation periods and faster loss of reliability during the crack propagation phase, which in turn implies faster damage accumulation.

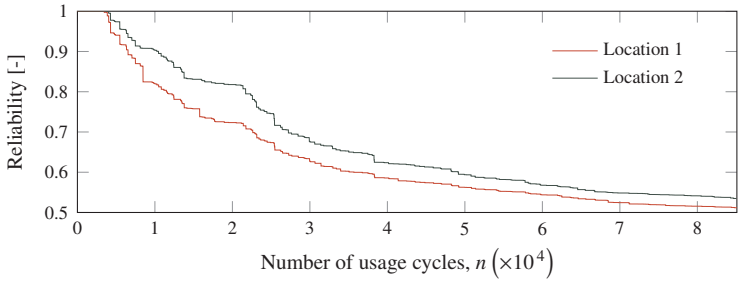

Figure 10: Evolution of reliability index at locations 1 and 2

5 CONCLUSIONS

This study presents a probabilistic framework for real-time reliability estimation of fatigue damage accumulation on wind turbine support structures. The approach is based on output-only measurements from wind turbine support structures and a combination of the augmented version of the Kalman filter with a fixed-lag smoother. The smoothed uncertainty of the estimated states is transferred through the FE model of the wind turbine substructure at the level of stresses and subsequently propagated over a stochastic non-stationary fatigue model for the identification of damage accumulation. The latter is finally obtained at unmeasured critical locations along with a time-dependent reliability index. Despite the fact that a strongly perturbed numerical model is implemented for the inverse problem, the structural quantities of interest are estimated with sufficiently high accuracy. This is mostly due to the capability of the algorithm to provide robust response predictions at the expense of the input estimates and partially due to the smoothing effect. However, it is seen that even a small amount of noise can give rise to spurious stress cycles and lead to an error accumulation on fatigue damage estimates.

ACKNOWLEDGEMENTS

The authors would like to gratefully acknowledge the support of the European Research Council via the ERC Starting Grant WINDMIL (ERC-2015-StG #679843) on the topic of Smart Monitoring, Inspection and Life-Cycle Assessment of Wind Turbines.

REFERENCES

[1] C. Papadimitriou, C. P. Fritzen, P. Kraemer, and E. Ntotsios. Fatigue predictions in entire body of metallic structures from a limited number of vibration sensors using Kalman filtering. *Structural Control and Health Monitoring*, 18:554–573, 2011.

[2] W. Schütz. A history of fatigue. *Engineering Fracture Mechanics*, 54(2):263–300, 1996.

[3] M. R. Saberi, A. R. Rahai, M. Sanayei, and R. M. Vogel. Bridge fatigue service-life estimation using operational strain measurements. *Journal of Bridge Engineering*, 21(5), 2016.

[4] H. Shen, J. Lin, and E. Mu. Probabilistic model on stochastic fatigue damage. *International Journal of Fatigue*, 22:569–572, 2000.

[5] V. Rathod, O. P. Yadav, A. Rathore, and R. Jain. Probabilistic modelling of fatigue damage accumulation for reliability prediction. *International Journal of Quality, Statistics and Reliability*, 2011.

[6] S. Thöns, M. H. Faber, and W. Rücker. Fatigue and Serviceability Limit State Model Basis for Assessment of Offshore Wind Energy Converters. *Journal of Offshore Mechanics and Arctic Engineering*, 134(3):031905–10, 2012.

[7] S. Thöns, R. Schneider, and M. H. Faber. Quantification of the value of Structural Health Monitoring information for fatigue deteriorating structural systems. In *12th International Conference on Applications of Statistics and Probability in Civil Engineering (ICASP12), Vancouver, Canada*, 2015.

[8] P. K. Kitanidis. Unbiased minimum-variance linear state estimation. *Automatica*, 23(6):775–778, 1987.

[9] S. Gillijns and B. De Moor. Unbiased minimum-variance input and state estimation for linear discrete-time systems with direct feedthrough. *Automatica*, 43:934–937, 2007.

[10] E. Lourens, C. Papadimitriou, S. Gillijns, E. Reynders, G. De Roeck, and G. Lombaert. Joint input-response estimation for structural systems based on reduced-order models and vibration data from a limited number of sensors. *Mechanical Systems and Signal Processing*, 29:310–327, 2012.

[11] E. Lourens, E. Reynders, G. De Roeck, G. Degrande, and G. Lombaert. An augmented Kalman filter for force identification in structural dynamics. *Mechanical Systems and Signal Processing*, 27:446–460, 2012.

[12] F. Naets, J. Cuadrado, and W. Desmet. Stable force identification in structural dynamics using Kalman filterign and dummy-measurements. *Mechanical Systems and Signal Processing*, 50-51:235–248, 2015.

[13] S. E. Azam, E. Chatzi, and C. Papadimitriou. A dual Kalman filter approach for state estimation via output-only acceleration measurements. *Mechanical Systems and Signal Processing*, 60-61:866–886, 2015.

[14] D. Simon. *Optimal State Estimation: Kalman, H Infinity, and Nonlinear Approaches*. Wiley-Interscience, 2006.

[15] A. Palmgren. Die lebensdauer von kugallagern. *VDI-Zeitschrift*, 68(14):416–425, 1924.

[16] M. A. Miner. Cumulative damage in fatigue. *ASME Applied Mechanics Transactions*, 12(3):159–164, 1945.

[17] S. Suresh. *Fatigue of materials*. Cambridge University Press, 1998.

[18] A. Wöhler. Versuche über die Festigkeit der Eisenbahnwagenachsen. *Zeitschrift für Bauwesen*, 10:160–161, 1860.

[19] W. F. Wu, H. Y. Liou, and H. C. Tse. Estimation of fatigue damage and fatigue life of components under random loading. *International Journal of Pressure Vessels and Piping*, 72(3):243–249, 1997.

[20] P. Wang and D. W. Coit. Reliability and degradation modelling with random or uncertain failure threshold. *Reliability and Maintainability Symposium*, pages 392–397, 2007.

[21] J. Jonkman, S Butterfield, W. Musial, and G. Scott. Definition of a 5-MW Reference Wind Turbine for Offshore System Development. Technical report, National Renewable Energy Laboratory (NREL), 2009.